Discovery of Novel *N*-Acylhydrazone Derivatives as Potent Inhibitors of Sirtuin-1

Victoria V. Lipson[*a,c]
Fedyr G. Yaremenko[a]
Volodymyr M. Vakula[a,b]
Svitlana V. Kovalenko[b]
Alexander V. Kyrychenko[b,c]
Sergiy M. Desenko[b]
Petro O. Borysko[d]
Sergiy O. Zozulya[d]

[a] State Institution 'V. Ya. Danilevsky Institute for Endocrine Pathology Problems', National Academy of Medical Sciences of Ukraine, Alchevsky St., 10, Kharkiv, 61002, Ukraine
lipson@ukr.net
[b] Division of Chemistry of Functional Materials, State Scientific Institution 'Institute for Single Crystals' NAS of Ukraine, 60 Nauky Ave., Kharkiv, 61072, Ukraine
[c] V.N. Karazin Kharkiv National University, 4 Svobody Sq., Kharkiv, 61022, Ukraine
[d] ENAMINE Ltd., Chervonotkatska str., 67, Kyiv, 02094, Ukraine

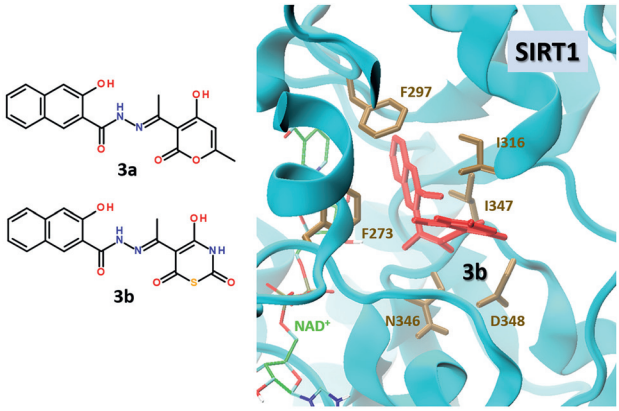

Received: 12.11.2023
Accepted: 11.03.2024
Published online: 04.04.2024 (Version of Record)
DOI: 10.1055/s-0043-1763747; Art ID: SO-2024-02-0010-OP

Abstract SIRT1 enzyme is a key family member of Silent Information Regulators (Sirtuins), which catalyze the deacetylation of proteins. Therefore, developing new SIRT1 inhibitors has potential application in treating cancer disease and age-related metabolic disorders. In this study, we synthesized a series of *N*-acylhydrazone (NAH) derivatives and performed high-throughput screening of their inhibitory activity against the recombinant SIRT1 protein by a luminescent assay. Using *in silico* screening, we identified a new NAH derivative that features both selectivity and a high binding affinity towards the active pocket of SIRT1 that are comparable to known inhibitors such as Ex527 and Sirtinol. Such high binding affinity makes the new derivatives promising alternatives to the available inhibitors and holds promise for developing better-targeted drugs against SIRT1 activity.

Key words Sirtuin1, organic synthesis, *N*-acylhydrazone, inhibitors, molecular docking

1 Introduction

In the last two decades, growing attention has been focused on epigenetic processes caused by cancer disease and age-related metabolic disorders, such as type 2 diabetes mellitus (T2DM), cancer, and cardiovascular and neurodegenerative diseases.[1–7] Epigenetic factors affect the functional activity of genes without altering the primary structure of their DNA. One of the mechanisms of gene regulation is mediated via posttranslational modification of proteins that form the histones essential for packaging chromosomal DNA.[8] Introducing acetyl groups into the structure of histone proteins by corresponding acetyltransferases leads to a reduction in their affinity to bind to DNA, and it becomes more accessible to a variety of transcription factors. In contrast, histone deacetylases (HDACs) remove acetyl residues and, as a result, DNA binds more tightly to histones.[9] Thus, DNA coding sequences are inaccessible to transcription factors and polymerases. Currently, both of these processes are of interest for the design of therapeutic agents capable of either inhibiting or activating the expression of certain genes.[10–12]

Intensively studied epigenetic factors are HDACs class III, so-called Sirtuins (SIRT1–7), which got their name from their homologous yeast Silent Information Regulator 2 (SIR2).[13–15] Sirtuins belong to a class of NAD^+-dependent deacetylase and are expressed in different subcellular compartments.[8] The most investigated SIRT1 is located both in the nucleus and the cytoplasm, and besides deacetylation of lysine residues in histones H1, H3, and H4 it performs many different functions.[16] At the moment, at least 35 protein targets for SIRT1 have been discovered, including various acetyltransferases, such as p300, p300/CBP-associated factor (PCAF), histone acetyltransferase (GCN5) complex with myogenic differentiation protein (MyoD), transcription factors p53, p65, Forkhead box proteins O1, 3a, and 4 (FoxOs), nuclear factor kappa B (NF-κB), sterol regulatory-binding protein 1c (SREBP-1c), peroxisome proliferator-activated receptor γ (PPARγ) and their co-activator 1α (PGC-1α),

AMP-activated protein kinase (AMPK) and many others that are involved in such cellular processes as differentiation, carbohydrate/lipid metabolism, mitochondrial biogenesis, inflammation, autophagy, stress resistance, apoptosis, provision circadian rhythms and 'silence' genes.[17–19] Listed transcription factors, co-regulators, and enzymes adapt gene expression and metabolic activity in response to the energy status of the cells. The latter is ensured through the involvement of NAD^+ as the cofactor for deacetylation, which is a unique feature of Sirtuins and not only provides a pathway for an association of enzyme activity with the metabolic (energy) status of the cell but also creates the possibility for external regulation.[8,9,20]

Thus, modulation of SIRT1 activity can be regarded as a promising strategy for treating metabolic disorders accompanied by diabetes mellitus type 2 (T2DM), cancer, neurodegenerative, and inflammatory diseases.[9,15] However, the presence of a large number of substrates for this HDAC leads to the need to solve the problem of selectivity for influence on certain processes in the case of using modulators of enzyme activity.[8] That is why, initially, most of the investigations related to the study of SIRT inhibitors among small organic molecules aimed to clarify the mechanisms of action of these deacetylases rather than using these compounds for pharmacological purposes.[7] Nevertheless, down-regulators of SIRTs have also recently been of great interest as potential agents in the treatment of cancer[8,21,22] and neurodegenerative disorders such as Parkinson's disease, Huntington's disease, Alzheimer's disease,[6,23,24] and human immunodeficiency virus.[25]

Over the past years, different SIRT inhibitors have been found among various classes of compounds.[7,26–32] Down-regulating activity towards HDACs class III was identified in 2-anilinobenzamides (nicotinamide analogues),[33] some acetyl lysine mimics,[26] azomethines based on 2-hydroxy-1-naphthaldehyde (sirtinol, JGB1714 and others analogues),[34,35] thioureas (cambinol, tenovin-6),[36,37] and thiobarbituric acid 5-ylidene derivatives,[38] bis(indolyl)maleinimides,[34] 5-benzylidene-2-phenyl-1,3-dioxane-4,6-diones[39] and indole derivatives,[40,41] naphtho[2,1-*b*]pyrane-3-ones (splitomicin and analogues),[42] thieno[3,2-*d*]pyrimidine-6-carboxamides,[43] 2-substituted nicotinic acid ethyl esters,[44] dihydro-1,4-benzoxazine carboxamides,[45] 1,5-dihydro-1*H*-pyrano[2,3-*d*]pyrimidine-2,4(3*H*)-diones,[46] dihydropyrano[2,3-*c*]pyrazole,[47] 2-arylamino-3-cyanopyridines,[48] 3-heteroarylmethylene isoindolin-1-ones,[49] 1,8-dioxo-octahydroxanthenes,[50] highly ionized naphthylurea suramin,[51] and various substances from natural sources (amurensin G)[52] or modified natural products such as steroids.[35] Most of these compounds have been evaluated using enzymatic and cell-based assays. Some of them are convenient tools for the investigation of ligand-bound complexes with different SIRTs, such as SIRT5-suramin X-ray crystal structure,[53] but only a few of them have been tested in animal models of cancer or other pathologies.[8,37]

Considering the currently available information on the activity of drug-like SIRT modulators, we synthesized some *N*-acylhydrazone (NAH) derivatives and their cyclic analogous – pyrazolines – by the methods given in our patent.[54] Bioactive NAH-based scaffolds have proven to be a very versatile and promising motif in drug design and medicinal chemistry.[55] Therefore, the design of this NAH derivative is based on both the known fragments specific for the HDACs class III down-regulators and the previously unexplored substituents. The inhibitory activity of the obtained compounds was evaluated by high-throughput screening against the recombinant SIRT1 protein. The binding mechanism and energetics of the new compounds were also examined by semiflexible molecular docking.

2 Results and Discussion

2.1 Chemistry

All target compounds **3a**,**b** and **10a–d** (Scheme 1) were synthesized according the methods described in our patent.[54] Hydrazones **3a**,**b** were obtained by interaction of hydrazine **1** with ketones **2a**,**b**. Pyrazolines **10a–d** (formally cyclic hydrazides) were synthesized by the reaction of carboxylic acids **4** and **5** with hydrazine **6** and unsaturated ketones **7–9** through preliminary formation of the corresponding hydrazides *in situ* (Scheme 1). The structure and composition of the obtained substances were confirmed by ^1H and ^{13}C NMR spectra, mass spectrometry, and elemental analysis. All characteristics of **3a–b** and **10a–d** correspond to those given in the patent.[54]

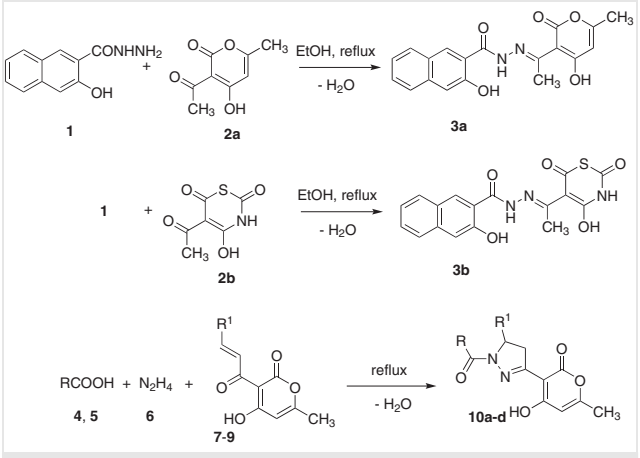

Scheme 1 Synthesis of compounds **3a**, **3b**, and **10a–d**. Compound **4**, **10a**,**b** R = CH_3; **5**, **10c**,**d** R = C_2H_5; **7**, **10a**,**c** R^1 = 4-HOC_6H_4, **8**, **10b** R^1 = 3,4-di(CH_3O)C_6H_3, **9**, **10d** R^1 = 4-$CH_3OC_6H_4$.

2.2 Molecular Docking Calculations

The crystallographic structure of SIRT1 (PDB ID: 4I5I) was used for the receptor. The graphical user interface of the AutoDock Tools (ADT) was employed to prepare the protein and ligands. A receptor grid box was 40×40×40 Å with a grid spacing of 0.375 Å, and a grid center positioned at Cartesian coordinates *x*=44.2, *y*=–20.7, and *z*=27.0. The AutoDock Vina 1.1.2 software was utilized for molecular docking calculations.[56,57] The protein receptor remained rigid throughout the docking process, while the ligand molecules were allowed to be flexible. Nine docking poses were obtained and ranked based on their score values in kcal/mol. Interaction analysis was performed using VMD and Discovery Studio Visualizer. Results with a positional root-mean-square deviation (RMSD) of less than 1.0 Å were clustered together and represented as the outcome with the most favorable free energy of binding. The pose with the lowest binding energy or binding affinity was extracted for further analysis.

2.3 *In Silico* Screening of Inhibitory Activity of *N*-Acylhydrazones Against SIRT1

The structural requirements for binding, modulating, and inhibiting of SIRT1 protein have been the subject of several recent studies, utilizing the available crystal structures of SIRT1 co-crystallized with known inhibitors.[45,58–60] The catalytic deacetylase region (residues 241–516) of SIRT1 is a key domain for governing the inhibitory activity of the full-length protein. The catalytic domain consists of a large classical Rossmann fold and a small zinc-binding domain (Figure 1).

It has been suggested that the acetylated peptide binds into the catalytic cleft between these two sub-domains and forms an enzyme–substrate complex.[51] Upon the SIRT1-catalyzed cleavage, the acetyl-lysine residue inserts into this conserved hydrophobic pocket. Co-factor NAD$^+$ plays a crucial role, and it is bound lengthwise across the binding pocket.[6] In the available SIRT1/NAD$^+$ crystal structure, the inhibitor Ex527 was deeply buried (Figure 1). Due to the well-characterized structure, the catalytic domain of SIRT1 has been used as a target receptor for *in silico* screening of binding parameters of SIRT1 modulators.[44–50,58,61–63]

To test whether our molecular docking approach is able to reproduce properly the correct binding mode of the co-crystallized inhibitor Ex527, we first re-docked it against the corresponding crystal structure of SIRT1 (PDB 4I5I).[58] It has been suggested that the presence of the co-factor NAD$^+$ was essential for the activity of the SIRT1 enzyme[45] so it was maintained in the binding site for the docking study. Figure 2 shows that the applied docking protocol was able to correctly reproduce the binding mode of the Ex527 inhibitor, which is closely overlapping with its corresponding crystallographic structure. Therefore, to estimate the inhibitory activity of the *N*-acylhydrazone derivatives, their structures were docked against the active pocket of the SIRT1 receptor utilizing the same docking settings.

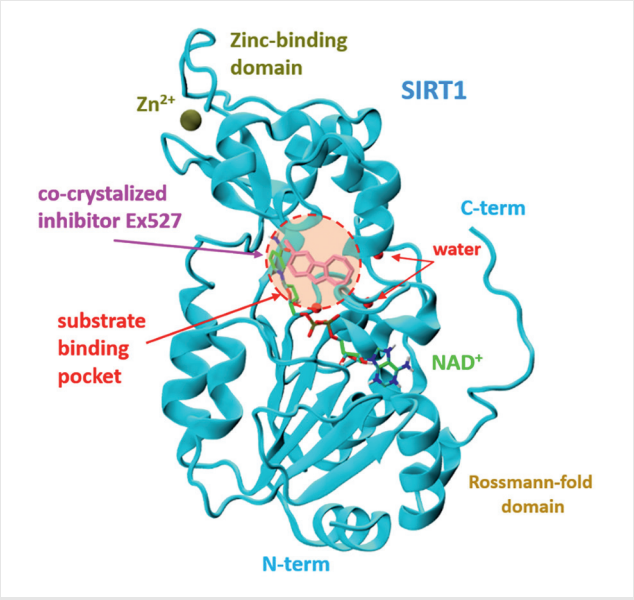

Figure 1 The 2.5 Å X-ray structure of the catalytic domain of SIRT1 (PDB 4I5I).[58] The co-crystallized inhibitor Ex527 is shown by the stick representation and colored magenta. The elongated lower pocket of the enzyme active site is occupied by the cofactor NAD$^+$. Zn^{2+} ion and three crystallized water molecules are displayed as balls.

Table 1 summarizes the binding affinity for the synthesized NAH derivatives against the crystal structure of SIRT1. To evaluate the role of co-factor NAD$^+$ and three co-crystal-

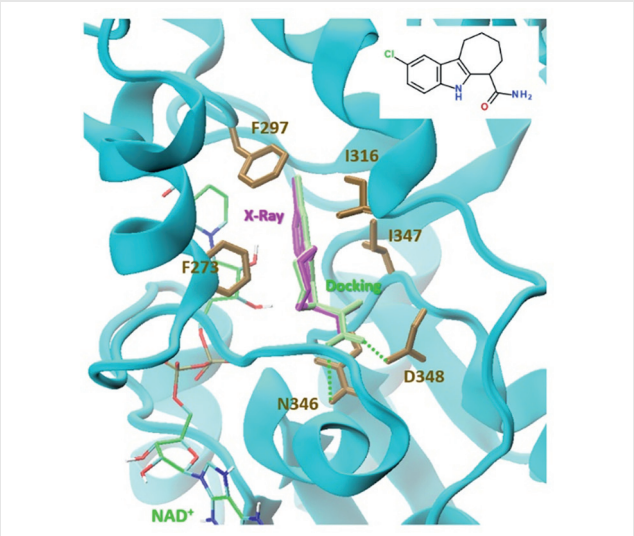

Figure 2 Structural comparison of binding mode of the co-crystallized ligand Ex527 (magenta) and its docked pose (green) within the binding pocket of SIRT1 (PDB-ID 4I5I). Crucial interactions with key amino acids N346 and D348 are shown with dotted lines.

lized water molecules (W702, W717, and W732), the molecular docking was carried out for three different receptor structures: (1) a free SIRT1 receptor, (2) SIRT1 receptor with the bound co-factor NAD+ (SIRT1/NAD+), (3) SIRT1 receptor with the bound co-factor NAD+ and crystal water molecules (SIRT1/NAD+/3W). In addition, to compare the binding affinity of the new NAH ligands, some existing inhibitors of SIRT1 with an IC_{50} in the range 0.048–120 μM (Figure 3) were also re-docked using the identical docking protocol.[8,26]

The molecular docking of the studied NAH derivatives and the known inhibitors (Table 1) revealed that the presence of bound co-factor NAD+ (SIRT1/NAD+) is critically important for proper binding of the ligands within the catalytic pocket of the enzyme. However, the addition of co-crystallized water molecules to the receptor structure (SIRT1/NAD+/3W) could lead to the loss of binding selectivity of existing inhibitors. It appears the co-crystallization of these water molecules is ligand-dependent and, therefore, they create some artificial steric effects for larger ligands (Table 1).

Our molecular docking results of the studied NAH derivatives showed that the ligands display a binding mode that is similar in many aspects to the well-known inhibitor Ex527 bound to the crystal structure of SIRT1 (Figure 4). The residue interaction analysis revealed that some of the nearest key residues, such as F273, I347, N346, and D348, are crucial for interaction with the bound inhibitors. These residues cover the ligand from the front- and side-faces and are involved in hydrophobic ligand–protein interactions. The same set of the active pocket residues of SIRT1 has been identified for binding recognition of other structurally diverse inhibitors.[28,46,47] Ligands **3a** and **3b** revealed high binding affinity from –9.5 to –9.6 kcal/mol towards the SIRT1/NAD+ receptor, which is of the same magnitude as the best-binding known inhibitors, such as Selermide and Sirtinol (see the Supporting Information, Figure S01). In terms of binding affinity, these ligands are better alternatives to other known inhibitors, such as Tenovin-1 and Tenovin-6 (Figure 3), as seen in Table 1.

Table 1 Comparison of the Inhibitory Potency of New *N*-Acylhydrazone Derivatives and Some Known Inhibitors Against SIRT1

Ligand	IC_{50} (μM)	Docking binding affinity (kcal/mol)		
		SIRT1	SIRT1/NAD+	SIRT1/NAD+/3W
Studied *N*-acylhydrazone derivatives				
3a	–	–11.8	–9.5	–9.0
3b	–	–10.9[a]	–9.6	–9.5
(*R*)-10a	–	–9.3[a]	–9.3	–8.7
(*S*)-10a	–	–10.1[a]	–7.7	–6.8[a]
(*R*)-10b	–	–8.9	–9.5	–6.5[a]
(*S*)-10b	–	–9.5[a]	–7.8	–6.8[a]
(*R*)-10c	–	–9.6[a]	–9.0	–7.2
(*S*)-10c	–	–9.8[a]	–7.4	–6.8[a]
(*R*)-10d	–	–9.4[a]	–9.4	–7.1[a]
(*S*)-10d	–	–9.3[a]	–7.9	–7.2[a]
Known inhibitors				
(*R*)-selisistat	–	–8.9	–10.0	–10.2
(*S*)-selisistat (Ex527)	0.048[45] 0.1[40,64]	–10.0	–10.7	–11.2
(*S*)-Indole 35	0.063[45] 0.12[40,64] 0.18[42]	–11.0	–11.8	–12.4
Salermide	76[64]	–10.6	–11.2	–10.2
Sirtinol	37.6[65] 120[42]	–11.6	–10.5	–6.4[a]
Tenovin-1	–	–10.3[a]	–9.4	–8.9
Tenovin-6	21[7] 100[42]	–10.0[a]	–8.6	–8.4
Sosbo 4.27	0.22[45]	–8.8	–8.5	–7.0[a]
Sosbo 4.2	1.48	–7.8	–7.4	–6.4[a]
Sosbo 4.22	0.15[45]	–8.8	–8.5	–6.9[a]

[a] A ligand is bound by an inactive out-of-pocket mode

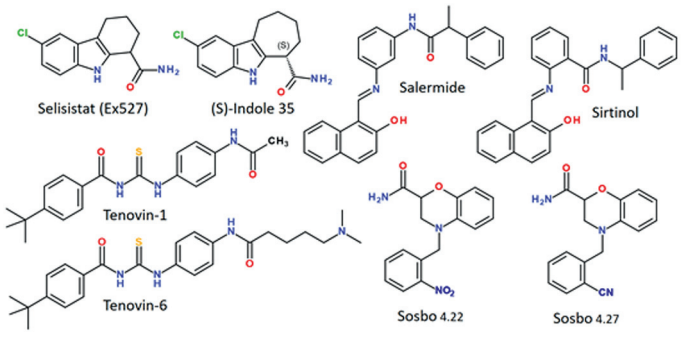

Figure 3 Chemical structure of some known inhibitors of SIRT1

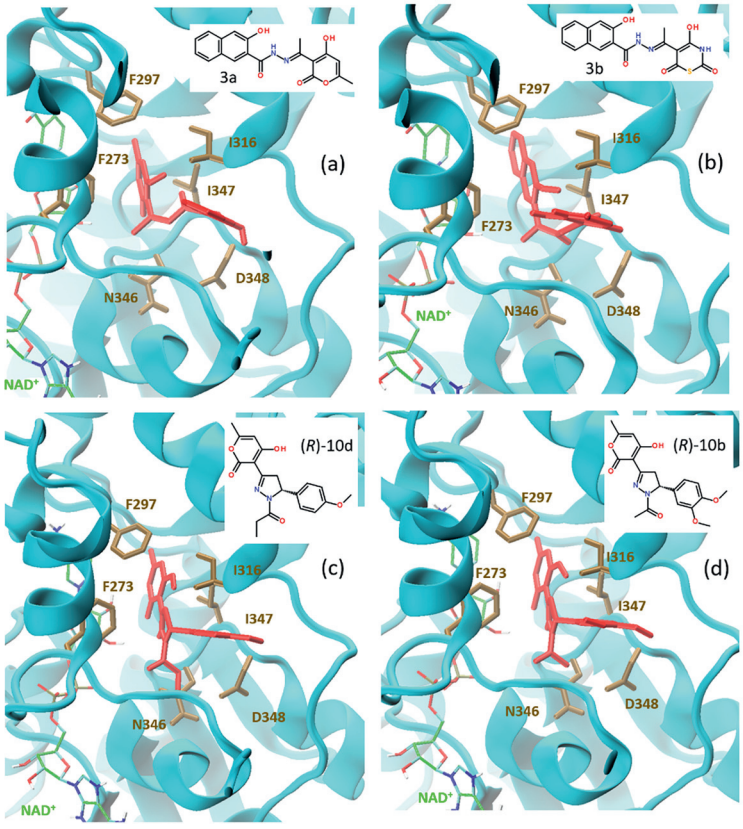

Figure 4 Molecular docking of the best binding ligands **3a**,**b**, **(*R*)-10d**, and **(*R*)-10b** into the active site of the SIRT1 enzyme

In addition, we found that for optically active ligands **3c–f** the binding properties of the two enantiomers differ significantly (Figure 5). The binding affinity of the *R*-enantiomer is essentially higher, being in a range from –9.3 to –9.5 kcal/mol, than that of the *S*-enantiomer, with the affinities in a range from –7.4 to –7.8 kcal/mol (Table 1).

2.4 High-Throughput Screening of Compounds 3a,b and 10a–d

The modulatory activity of acylhydrazone derivatives were determined with recombinant SIRT1 protein using the mode of high-throughput screening by detecting a luminogenic product with the SIRT-Glo™ Assay kit (Cat. G6450) manufactured by Promega (Madison, USA).[66] Recombinant Sirtuin1 protein manufactured by SignalChem (Cat. S35-31H-10) was used.

Weights of substances were dissolved in dimethyl sulfoxide (DMSO) and then added to the reaction buffer in the amount of 80 µM (the final concentration of substances in the reaction mixture was 20 µM, the final concentration of DMSO in the test was 1%). The test compounds were added in 25 µL to a well of a 96-well plate. Nicotinamide (cat. G6540) was used as a reference inhibitor compound at a final concentration of 250 µM (1% DMSO). In the next step, 25 µL of Sirtuin1 protein at a concentration of 0.4 ng/µL (2 ng of protein per well in a reaction volume of 10 µL of a

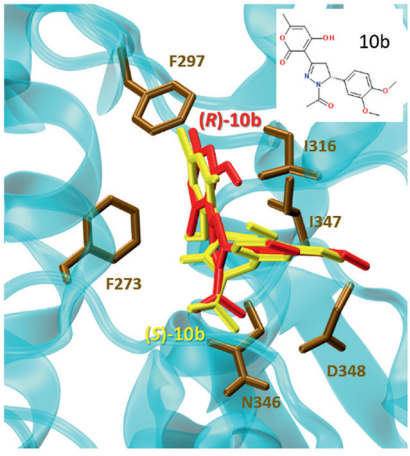

Figure 5 Superimposition of the two docked poses of **(*R*)-10b** (red sticks) and **(*S*)-10b** (yellow sticks) bound to the active pocket of SIRT1. The key nearest amino acids interacting with the ligands are depicted as brown sticks. Co-factor NAD^+ is not shown for clarity.

384-well plate) was added. The pre-reaction mixture was incubated for 30 min at room temperature (25 °C). After that, the mixture was transferred from a 96-well plate to a small-volume 384-well white plate manufactured by Corning (cat. 3673) in 10 µL portions, in four replicates.

To initiate the enzymatic reaction, 10 µL of SIRT-Glo™ reagent (a mixture of SIRT-Glo™ Substrate, cat. G644A and Developer Reagent, cat. G644B, according to the protocol[65]) was added to the pre-reaction mixture. The reaction mixture was incubated at room temperature for 40 min. Luminescence was read using an Omega PolarStar microplate reader. The percentage of inhibition was determined from Equation 1:

$$\text{Inhibition}(\%) = 100 - \left(\left(\frac{X - \text{Aver}_{min}}{(\text{Aver}_{max} - \text{Aver}_{min})}\right)*100\right) \quad (1)$$

Equation 1

where X is the luminescence signal at the test point, Aver_{min} is the arithmetic mean of the luminescence of the negative control (reaction without the addition of protein), and Aver_{max} is the arithmetic mean value of the luminescence of the positive control (reaction with the addition of protein, but without the addition of modulator compounds). The inhibition percentage was calculated for each point separately, and then the arithmetic mean of four replicates of the reaction was found for each compound. The inhibition rates of the test compounds are summarized in Table 2.

Table 2 The SIRT1 Modulatory Activity of NAH Derivatives **3a**,**b** and **10a–d**

Compound	3a	3b	10a	10b	10c	10d
Inhibition of SIRT1 at a concentration of 20 µM (%)	90	100	8	–3[a]	97	–4[a]

[a] Activation of SIRT1 in %.

3 Conclusions

The *N*-acylhydrazone scaffold was explored for the synthesis of novel derivatives as potential inhibitors of SIRT1 enzyme. High-throughput screening of compounds **3a**,**b** and **10a–d** using a luminescent assay demonstrated the highest inhibitory rates for derivative **3b**. The semiflexible molecular docking corroborates these results and suggests that the binding mode of the studied derivatives **3a** and **3b** into the active pocket of SIRT1 is similar to that of the known inhibitor Ex527. Compounds **3a** and **3b** act as non-covalent inhibitors that bind to the enzyme–substrate complex with a binding affinity that is comparable to the affinity of hit-inhibitors of this family, such as Sirtinol. Moreover, enantiomers of ligands **10a–d** revealed the binding stereoselectivity of the *R*-enantiomer over the *S*-enantiomer. Finally, our findings hold promise that the synthesized NAH derivatives can be used for developing highly potent inhibitors against SIRT1 enzymes.

All commercially available reagents and solvents were purchased from Sigma Aldrich and used without further purification. ^{1}H NMR spectra were recorded with a Bruker AM-300 spectrometer 300 MHz, ^{13}C NMR spectra were recorded with a Varian MR-400 spectrometer 100 MHz, with TMS as an internal standard in all cases and DMSO-d_6+CCl_4 or DMSO-d_6 as solvents. All chemical shift values are reported in units of δ (ppm). The mass spectra were recorded with a Varian 1200L GC–MS instrument or with a Varian MAT CH-6, ionization by EI at 70 eV. Elemental analyses were carried out with an EA 3000 Eurovector elemental analyzer. Melting points were determined with a Kofler hot bench and are uncorrected. The progress of reactions and the purity of the obtained compounds were monitored by TLC on Alugrams Xtra SIL G/UV254 plates with chloroform–ethanol (24:1) as eluent.

3-Hydroxy-*N*′-[(1*E*)-1-(6-methyl-2,4-dioxo-2*H*-pyran-3(4*H*)-ylidene)ethyl]-2-naphthohydrazide (3a)

To a solution of 3-hydroxy-2-naphthohydrazide (0.3 g, 1.48 mmol) in a mixture of EtOH-DMF (10:1), dehydroacetic acid (DHA; 0.25 g, 1.49 mmol) was added and heated at reflux until a precipitate formed. The target compound **3a** was filtered off and washed with EtOH.

Yield: 0.45 g (86 %); yellow crystal powder; mp 263–264 °C.[54]

^{1}H NMR (300 MHz, DMSO-d_6): δ = 16.1 (bs, 1 H, OH), 11.3 (bs, 2 H, 2×NH), 8.48 (s, 1 H, C^2′H), 7.94 (d, *J* = 7.9 Hz, 1 H, C^3′H), 7.76 (d, *J* = 8.2 Hz, 1 H, C^6′H), 7.52 (t, *J* = 7.6 Hz, 1 H, C^5′H), 7.36 (t, *J* = 7.6 Hz, 1 H, C^4′H), 7.34 (s, 1 H, C^7′H), 5.92 (s, 1 H, C^{5}H), 2.66 (s, 3 H, CH_3), 2.15 (s, 3 H, CH_3).

^{13}C NMR (126 MHz, DMSO-d_6): δ = 181.4, 168.4, 163.7, 163.6, 162.8, 153.4, 136.4, 132.1, 129.3, 128.8, 127.3, 126.2, 124.3, 120.3, 110.9, 105.9, 95.3, 19.7, 17.1.

MS: *m*/*z* (%) = 352 (8) [M], 182 (8), 172 (12), 171 (100), 170 (35), 142 (19), 115 (71), 114 (16), 85 (14), 69 (13), 67 (11), 55 (10), 44 (17).

Anal Calcd. for $C_{19}H_{16}N_2O_5$: C, 64.77; H, 4.58; N, 7.95. Found: C, 64.85; H, 4.54; N, 7.88.

3-Hydroxy-*N*′-[(1*E*)-1-(2,4,6-trioxo-1,3-thiazinan-5-ylidene)ethyl]-2-naphthohydrazide (3b)

To a solution of 5-acetyl-4-hydroxy-2*H*-1,3-thiazine-2,6(3*H*)-dione (0.3 g, 1.6 mmol) in EtOH (8 mL) a solution of 3-hydroxy-2-naphthohydrazide (0.32 g, 1.6 mmol) in EtOH (10 mL) was added and the reaction mixture was heated at reflux until a precipitate formed. The target compound **3b** was filtered off and washed with EtOH.

Yield: 0.39 g (65 %); yellow crystal powder; mp 224–225 °C.[54]

^{1}H NMR (200 MHz, DMSO-d_6): δ = 14.3 (bs, 1 H, OH), 11.83 (s, 1 H, NH), 8.45 (s, 1 H, C^2′H), 7.95 (d, *J* = 7.9 Hz, 1 H, C^3′H), 7.76 (d, *J* = 8.0 Hz, 1 H, C^6′H), 7.52 (dt, J_1 = 7.8 Hz, J_2 = 1.1 Hz, 1 H, C^5′H), 7.35 (dt, J_1 = 7.4 Hz, J_2 = 1.0 Hz, 1 H, C^4′H), 7.32 (s, 1 H, C^7′H), 2.66 (s, 3 H, CH_3).

^{13}C NMR (126 MHz, DMSO-d_6): δ = 180.6, 170.2, 168.2, 164.6, 163.7, 153.6, 136.4, 131.9, 129.2, 128.9, 127.3, 126.2, 124.3, 120.2, 110.9, 96.1, 18.4.

MS: *m*/*z* (%) = 371 (4) [M], 370 (32), 310 (8), 267 (54), 248 (42), 224 (17), 212 (8), 186 (12), 143 (37), 140 (55), 97 (100).

Anal. Calcd. for $C_{17}H_{13}N_3O_5S$: C, 54.98; H, 3.53; N, 11.31; S, 8.63. Found: C, 55.08; H, 3.50; N, 11.27; S, 8.71.

3-[1-Acetyl-5-(4-hydroxyphenyl)-4,5-dihydro-1*H*-pyrazol-3-yl]-4-hydroxy-6-methyl-2*H*-pyran-2-one (10a)

Hydrazine hydrate (0.15 mL) was added dropwise to a solution of 4-hydroxy-3-[(2*E*)-3-(4-hydroxyphenyl)prop-2-enoyl]-6-methyl-2*H*-pyran-2-one (0.34 g, 1.25 mmol) in acetic acid (15 mL) and the reaction mixture was heated at reflux until the disappearance of the initial unsaturated ketone (TLC monitoring). After cooling, the reaction mixture was stirred with ice and the precipitate of compound **10a** was filtered off and washed with water. The target compound was purified by crystallization from $CHCl_3$–EtOH (10:1).

Yield: 0.33 g (80%); cream crystal powder; mp 263–266 °C.[54]

^{1}H NMR (300 MHz, DMSO-d_6+CCl_4): δ = 12.58 (s, 1 H, OH), 9.08 (s, 1 H, OH), 6.98 (d, *J* = 8.0 Hz, 2H, Ar), 6.68 (d, *J* = 8.0 Hz, 2 H, Ar), 6.23 (s, 1 H, CH_{pyr}), 5.34 (dd, J_1 = 11.8 Hz, J_2 = 2.5 Hz, 1 H, C^5H_{Przl}), 3.86 (dd, J_1 = 19.0 Hz, J_2 = 11.8 Hz, 1H, $C^4H^1{}_{przl}$), 3.30 (dd, J_1 = 19.2 Hz, J_2 = 2.0 Hz, 1 H, $C^4H^2{}_{przl}$), 2.26 (s, 3 H, $COCH_3$), 2.22 (s, 3 H, CH_{3pyr}).

^{13}C NMR (126 MHz, DMSO-d_6): δ = 171.2, 166.9, 165.6, 161.7, 157.0, 155.1, 132.8, 127.2, 115.7, 100.9, 94.1, 57.5, 45.6, 22.2, 20.1.

MS: *m*/*z* (%) = 328 (5) [M], 327 (46), 244 (10), 243 (100), 241 (6), 123 (40), 66 (25).

Anal. cacld. for $C_{17}H_{16}N_2O_5$: C, 62.19; H, 4.91; N, 8.53. Found: C, 62.32; H, 4.90; N, 8.47.

3-[1-Acetyl-5-(3,4-dimethoxyphenyl)-4,5-dihydro-1*H*-pyrazol-3-yl]-4-hydroxy-6-methyl-2*H*-pyran-2-one (10b)

Yield: 0.35 g (78 %); cream powder; mp 165–167 °C.[54]

^{1}H NMR (300 MHz, DMSO-d_6+CCl_4): δ = 12.56 (s, 1 H, OH), 6.83 (d, *J* = 8.3 Hz, 1 H, $C^{5'}H$), 6.78 (s, 1 H, $C^{2'}H$), 6.68 (d, *J* = 8.0 Hz, 1 H, $C^{6'}H$), 6.23 (s, 1 H, CH_{pyr}), 5.30–5.44 (m, 1 H, C^5H_{przl}), 3.81 (m, 1 H, $C^4H^1{}_{przl}$), 3.78 (s, 3 H, OCH_3), 3.76 (s, 3 H, OCH_3), 3.25–3.37 (m, 1 H, $C^4H^2{}_{przl}$), 2.27 (s, 3 H, CH_3), 2.24 (s, 3 H, CH_{3pyr}).

^{13}C NMR (126 MHz, DMSO-d_6): δ = 171.1, 167.0, 165.6, 161.8, 154.9, 149.2, 148.4, 134.9, 117.5, 112.2, 109.9, 100.8, 94.1, 57.8, 55.9, 55.9, 45.6, 22.2, 20.1.

MS: *m*/*z* (%) = 372 (6) [M], 368 (8), 327 (9), 288 (9), 287 (100), 209 (4), 127 (19), 66 (9).

Anal. Calcd. for $C_{19}H_{20}N_2O_6$: C, 61.28; H, 5.41; N, 7.52. Found: C, 61.17; H, 5.48; N, 7.57.

4-Hydroxy-3-[5-(4-hydroxyphenyl)-1-propionyl-4,5-dihydro-1*H*-pyrazol-3-yl]-6-methyl-2*H*-pyran-2-one (10c)

Hydrazine hydrate (0.15 mL) was added dropwise to a solution of 4-hydroxy-3-[(2*E*)-3-(4-hydroxyphenyl)prop-2-enoyl]-6-methyl-2*H*-pyran-2-one (0.34 g, 1.25 mmol) in propionic acid (13 mL). The reaction mixture was heated at reflux until the disappearance of the initial unsaturated ketone (TLC monitoring). After cooling, the reaction mixture was stirred with ice and the precipitate of compound **10c** was filtered off and washed with water. The target compound was purified by crystallization from mixture of $CHCl_3$–EtOH (8:1).

Yield: 0.30 g (70%); cream crystal powder; mp 264–266 °C.[54]

^{1}H NMR (300 MHz, DMSO-d_6): δ = 9.29 (s, 1 H, OH), 7.59–7.62 (m, 1 H, OH), 7.00 (d, *J* = 8.6 Hz, 2 H, Ar), 6.70 (d, *J* = 8.0 Hz, 2 H, Ar), 6.30 (s, 1 H, CH_{pyr}), 5.34 (d, *J* = 7.8 Hz, 1 H, C^5H_{przl}), 3.84 (dd, J_1 = 18.9 Hz, J_2 = 12.0 Hz, 1 H, $C^4H^1{}_{przl}$), 3.50–4.00 (m, 1 H, $C^4H^2{}_{Przl}$), 2.54–2.65 (m, 2 H, $COCH_2$), 2.24 (s, 3H, CH_{3pyr}), 0.95–1.07 (m, 3 H, CH_3).

^{13}C NMR (126 MHz, DMSO-d_6): δ = 171.1, 170.0, 165.6, 161.7, 157.0, 155.0, 132.9, 127.1, 115.7, 100.8, 94.1, 57.6, 45.3, 27.2, 20.1, 9.1.

MS: *m*/*z* (%) = 342 (5) [M], 341 (24), 258 (8), 257 (100), 241 (6), 137 (26), 96 (19), 66 (30).

Anal. Calcd. for $C_{18}H_{18}N_2O_5$: C, 63.15; H, 5.30; N, 8.18. Found: C, 63.02; H, 5.37; N, 8.22.

4-Hydroxy-3-[5-(4-methoxyphenyl)-1-propionyl-4,5-dihydro-1*H*-pyrazol-3-yl]-6-methyl-2*H*-pyran-2-one (10d)

Yield: 0.3 g (70 %); cream powder; mp 173–176 °C.[54]

^{1}H NMR (300 MHz, DMSO-d_6): δ = 7.13 (d, *J* = 8.3 Hz, 2 H, Ar), 6.88 (d, *J* = 8.4 Hz, 2 H, Ar), 6.29 (s, 1 H, CH_{pyr}), 5.39 (d, *J* = 11.2 Hz, 1 H, C^5H_{przl}), 3.87 (dd, J_1 = 17.8 Hz, J_2 = 11.0 Hz, 1 H, $C^4H^1{}_{przl}$), 3.73 (s, 3 H, OCH_3), 3.0–3.4 (m, 1 H, $C^4H^2{}_{przl}$), 2.54–2.66 (m, 2 H, $COCH_2$), 2.24 (s, 3 H, CH_{3pyr}), 1.03 (t, *J* = 6.4 Hz, 3 H, CH_3).

^{13}C NMR (126 MHz, DMSO-d_6): δ = 170.7, 169.6, 165.1, 161.2, 158.4, 154.4, 134.1, 126.7, 113.9, 100.3, 93.6, 57.1, 55.0, 44.8, 26.7, 19.5, 8.5.

MS: *m*/*z* (%) = 357 (11), 356 (48) [M], 300 (38), 299 (74), 284 (7), 249 (8), 216 (12), 215 (20), 194 (14), 193 (100), 192 (13), 166 (15), 134 (15), 128 (10), 121 (15), 115 (19), 109 (20), 91 (12), 85 (24), 77 (15), 57 (89).

Anal. Calcd. for $C_{19}H_{20}N_2O_5$: C, 64.03; H, 5.66; N, 7. 86. Found: C, 64.05; H, 5.60; N, 7.92.

Conflict of Interest

The authors declare no conflict of interest.

Funding Information

The authors acknowledge the National Academy of Science of Ukraine for financial support under the project 0122U001857 and the National Academy of Medical Science of Ukraine for financial support under the project 0121U111536.

Supporting Information

Supporting information for this article is available online at https://doi.org/10.1055/s-0043-1763747.

References

(1) Baylin, S. B.; Jones, P. A. *Nat. Rev. Cancer* **2011**, *11*, 726.
(2) Yoo, C. B.; Jones, P. A. *Nat. Rev. Drug Discovery* **2006**, *5*, 37.
(3) Jones, P. A.; Baylin, S. B. *Cell* **2007**, *128*, 683.
(4) Teixeira, C. S. S.; Cerqueira, N. M. F. S. A.; Gomes, P.; Sousa, S. F. *Int. J. Mol. Sci.* **2020**, *21*, 8609.
(5) Nightingale, K. P.; O'Neill, L. P.; Turner, B. M. *Curr. Opin. Genet. Dev.* **2006**, *16*, 125.
(6) Lavu, S.; Boss, O.; Elliott, P. J.; Lambert, P. D. *Nat. Rev. Drug Discovery* **2008**, *7*, 841.
(7) Kumar, A.; Chauhan, S. *Eur. J. Med. Chem.* **2016**, *119*, 45.
(8) Wu, Q.-J.; Zhang, T.-N.; Chen, H.-H.; Yu, X.-F.; Lv, J.-L.; Liu, Y.-Y.; Liu, Y.-S.; Zheng, G.; Zhao, J.-Q.; Wei, Y.-F.; Guo, J.-Y.; Liu, F.-H.; Chang, Q.; Zhang, Y.-X.; Liu, C.-G.; Zhao, Y.-H. *Signal Transduction Targeted Ther.* **2022**, *7*, 402.

(9) Wang, T.; Wang, Y.; Liu, L.; Jiang, Z.; Li, X.; Tong, R.; He, J.; Shi, J. *Eur. J. Med. Chem.* **2020**, *193*, 112207.
(10) Gregoretti, I.; Lee, Y.-M.; Goodson, H. V. *J. Mol. Biol.* **2004**, *338*, 17.
(11) Falkenberg, K. J.; Johnstone, R. W. *Nat. Rev. Drug Discovery* **2014**, *13*, 673.
(12) Ruijter, A. J. M. d.; Gennip, A. H. v.; Caron, H. N.; Kemp, S.; Kuilenburg, A. B. P. v. *Biochem. J.* **2003**, *370*, 737.
(13) Blander, G.; Guarente, L. *Annu. Rev. Biochem.* **2004**, *73*, 417.
(14) Feldman, J. L.; Dittenhafer-Reed, K. E.; Denu, J. M. *J. Biol. Chem.* **2012**, *287*, 42419.
(15) Nandave, M.; Acharjee, R.; Bhaduri, K.; Upadhyay, J.; Rupanagunta, G. P.; Ansari, M. N. *Int. J. Biol. Macromol.* **2023**, *242*, 124581.
(16) Sauve, A. A.; Wolberger, C.; Schramm, V. L.; Boeke, J. D. *Annu. Rev. Biochem.* **2006**, *75*, 435.
(17) Yamamoto, H.; Schoonjans, K.; Auwerx, J. *Mol. Endocrinol.* **2007**, *21*, 1745.
(18) Cantó, C.; Auwerx, J. *Curr. Opin. Lipidol.* **2009**, *20*, 98.
(19) Lan, F.; Cacicedo, J. M.; Ruderman, N.; Ido, Y. *J. Biol. Chem.* **2008**, *283*, 27628.
(20) Zhang, T.; Kraus, W. L. *Biochim. Biophys. Acta* **2010**, *1804*, 1666.
(21) Villalba, J. M.; Alcaín, F. J. *BioFactors* **2012**, *38*, 349.
(22) Mellini, P.; Valente, S.; Mai, A. *Expert Opin. Ther. Pat.* **2015**, *25*, 5.
(23) Fischer, A.; Sananbenesi, F.; Mungenast, A.; Tsai, L.-H. *Trends Pharmacol. Sci.* **2010**, *31*, 605.
(24) Kratz, E. M.; Sołkiewicz, K.; Kubis-Kubiak, A.; Piwowar, A. *Int. J. Mol. Sci.* **2021**, *22*, 630.
(25) Pagans, S.; Pedal, A.; North, B. J.; Kaehlcke, K.; Marshall, B. L.; Dorr, A.; Hetzer-Egger, C.; Henklein, P.; Frye, R.; McBurney, M. W.; Hruby, H.; Jung, M.; Verdin, E.; Ott, M. *PLoS Biol.* **2005**, *3*, e41.
(26) Chen, L. *Curr. Med. Chem.* **2011**, *18*, 1936.
(27) Abbotto, E.; Scarano, N.; Piacente, F.; Millo, E.; Cichero, E.; Bruzzone, S. *Molecules* **2022**, *27*, 5641.
(28) Purushotham, N.; Singh, M.; Paramesha, B.; Kumar, V.; Wakode, S.; Banerjee, S. K.; Poojary, B.; Asthana, S. *RSC Adv.* **2022**, *12*, 3809.
(29) Kumar, R.; Nigam, L.; Singh, A. P.; Singh, K.; Subbarao, N.; Dey, S. *Eur. J. Med. Chem.* **2017**, *127*, 909.
(30) Wu, J.; Zhang, D.; Chen, L.; Li, J.; Wang, J.; Ning, C.; Yu, N.; Zhao, F.; Chen, D.; Chen, X.; Chen, K.; Jiang, H.; Liu, H.; Liu, D. *J. Med. Chem.* **2013**, *56*, 761.
(31) Han, H.; Li, C.; Li, M.; Yang, L.; Zhao, S.; Wang, Z.; Liu, H.; Liu, D. *Molecules* **2020**, *25*, 2755.
(32) Yang, L.-L.; Wang, H.-L.; Yan, Y.-H.; Liu, S.; Yu, Z.-J.; Huang, M.-Y.; Luo, Y.; Zheng, X.; Yu, Y.; Li, G.-B. *Eur. J. Med. Chem.* **2020**, *192*, 112201.
(33) Suzuki, T.; Imai, K.; Nakagawa, H.; Miyata, N. *ChemMedChem* **2006**, *1*, 1059.
(34) Botta, G. P.; De Santis, L.; Saladino, R. *Curr. Med. Chem.* **2012**, *19*, 5871.
(35) Grozinger, C. M.; Chao, E. D.; Blackwell, H. E.; Moazed, D.; Schreiber, S. L. *J. Biol. Chem.* **2001**, *276*, 38837.
(36) Heltweg, B.; Gatbonton, T.; Schuler, A. D.; Posakony, J.; Li, H.; Goehle, S.; Kollipara, R.; DePinho, R. A.; Gu, Y.; Simon, J. A.; Bedalov, A. *Cancer Res.* **2006**, *66*, 4368.
(37) Lain, S.; Hollick, J. J.; Campbell, J.; Staples, O. D.; Higgins, M.; Aoubala, M.; McCarthy, A.; Appleyard, V.; Murray, K. E.; Baker, L.; Thompson, A.; Mathers, J.; Holland, S. J.; Stark, M. J. R.; Pass, G.; Woods, J.; Lane, D. P.; Westwood, N. J. *Cancer Cell* **2008**, *13*, 454.
(38) Uciechowska, U.; Schemies, J.; Neugebauer, R. C.; Huda, E.-M.; Schmitt, M. L.; Meier, R.; Verdin, E.; Jung, M.; Sippl, W. *ChemMedChem* **2008**, *3*, 1965.
(39) Li, C.; Hu, S.-S.; Yang, L.; Wang, M.; Long, J.-D.; Wang, B.; Han, H.; Zhu, H.; Zhao, S.; Liu, J.-G.; Liu, D.; Liu, H. *ACS Med. Chem. Lett.* **2021**, *12*, 397.
(40) Napper, A. D.; Hixon, J.; McDonagh, T.; Keavey, K.; Pons, J.-F.; Barker, J.; Yau, W. T.; Amouzegh, P.; Flegg, A.; Hamelin, E.; Thomas, R. J.; Kates, M.; Jones, S.; Navia, M. A.; Saunders, J. O.; DiStefano, P. S.; Curtis, R. *J. Med. Chem.* **2005**, *48*, 8045.
(41) Laaroussi, H.; Ding, Y.; Teng, Y.; Deschamps, P.; Vidal, M.; Yu, P.; Broussy, S. *Eur. J. Med. Chem.* **2020**, *202*, 112561.
(42) Sanders, B. D.; Jackson, B.; Brent, M.; Taylor, A. M.; Dang, W.; Berger, S. L.; Schreiber, S. L.; Howitz, K.; Marmorstein, R. *Bioorg. Med. Chem.* **2009**, *17*, 7031.
(43) Disch, J. S.; Evindar, G.; Chiu, C. H.; Blum, C. A.; Dai, H.; Jin, L.; Schuman, E.; Lind, K. E.; Belyanskaya, S. L.; Deng, J.; Coppo, F.; Aquilani, L.; Graybill, T. L.; Cuozzo, J. W.; Lavu, S.; Mao, C.; Vlasuk, G. P.; Perni, R. B. *J. Med. Chem.* **2013**, *56*, 3666.
(44) Challa, C. S.; Katari, N. K.; Nallanchakravarthula, V.; Nayakanti, D.; Kapavarapu, R.; Pal, M. *J. Mol. Struct.* **2021**, *1245*, 131069.
(45) Spinck, M.; Bischoff, M.; Lampe, P.; Meyer-Almes, F.-J.; Sievers, S.; Neumann, H. *J. Med. Chem.* **2021**, *64*, 5838.
(46) Kondabanthini, S.; Akshinthala, P.; Katari, N. K.; Srimannarayana, M.; Gundla, R.; Kapavarapu, R.; Pal, M. *J. Mol. Struct.* **2023**, *1276*, 134753.
(47) Kondabanthini, S.; Katari, N. K.; Srimannarayana, M.; Gundla, R.; Kapavarapu, R.; Pal, M. *J. Mol. Struct.* **2022**, *1266*, 133527.
(48) Challa, C. S.; Katari, N. K.; Nallanchakravarthula, V.; Nayakanti, D.; Kapavarapu, R.; Pal, M. *J. Mol. Struct.* **2022**, *1253*, 132309.
(49) Ganapathisivaraja, P.; Rao, G. V. N.; Ramarao, A.; Tej, M. B.; Praneeth, M. S.; Kapavarapu, R.; Rao, M. V. B.; Pal, M. *J. Mol. Struct.* **2022**, *1250*, 131788.
(50) Manikanttha, M.; Deepti, K.; Tej, M. B.; Reddy, A. G.; Kapavarapu, R.; Rao, M. V. B.; Pal, M. *J. Mol. Struct.* **2022**, *1264*, 133313.
(51) Trapp, J.; Meier, R.; Hongwiset, D.; Kassack, M. U.; Sippl, W.; Jung, M. *ChemMedChem* **2007**, *2*, 1419.
(52) Oh, W. K.; Cho, K. B.; Hien, T. T.; Kim, T. H.; Kim, H. S.; Dao, T. T.; Han, H.-K.; Kwon, S.-M.; Ahn, S.-G.; Yoon, J.-H.; Kim, T. H.; Kim, Y. G.; Kang, K. W. *Mol. Pharmacol.* **2010**, *78*, 855.
(53) Schuetz, A.; Min, J.; Antoshenko, T.; Wang, C.-L.; Allali-Hassani, A.; Dong, A.; Loppnau, P.; Vedadi, M.; Bochkarev, A.; Sternglanz, R.; Plotnikov, A. N. *Structure* **2007**, *15*, 377.
(54) Yaremenko, F. G.; Vakula, V. M.; Svydlo, I. M.; Borodina, V. V.; Borisko, P. O.; Zozulya, S. O.; Grynukova, A. B. UA Patent 121892, **2020**.
(55) Thota, S.; Rodrigues, D. A.; Pinheiro, P. d. S. M.; Lima, L. M.; Fraga, C. A. M.; Barreiro, E. J. *Bioorg. Med. Chem. Lett.* **2018**, *28*, 2797.
(56) Trott, O.; Olson, A. J. *J. Comput. Chem.* **2010**, *31*, 455.
(57) Goodsell, D. S.; Sanner, M. F.; Olson, A. J.; Forli, S. *Protein Sci.* **2021**, *30*, 31.
(58) Zhao, X.; Allison, D.; Condon, B.; Zhang, F.; Gheyi, T.; Zhang, A.; Ashok, S.; Russell, M.; MacEwan, I.; Qian, Y.; Jamison, J. A.; Luz, J. G. *J. Med. Chem.* **2013**, *56*, 963.
(59) Dai, H.; Case, A. W.; Riera, T. V.; Considine, T.; Lee, J. E.; Hamuro, Y.; Zhao, H.; Jiang, Y.; Sweitzer, S. M.; Pietrak, B.; Schwartz, B.; Blum, C. A.; Disch, J. S.; Caldwell, R.; Szczepankiewicz, B.; Oalmann, C.; Yee, Ng. P.; White, B. H.; Casaubon, R.; Narayan, R.; Koppetsch, K.; Bourbonais, F.; Wu, B.; Wang, J.; Qian, D.; Jiang, F.; Mao, C.; Wang, M.; Hu, E.; Wu, J. C.; Perni, R. B.; Vlasuk, G. P.; Ellis, J. L. *Nat. Commun.* **2015**, *6*, 7645.

(60) Karaman, B.; Jung, M.; Sippl, W. *Structure-Based Design and Computational Studies of Sirtuin Inhibitors*, In *Epi-informatics*; Medina-Franco, J. L., Ed.; Academic Press: Boston, **2016**, 297–325.
(61) Mai, A.; Valente, S.; Meade, S.; Carafa, V.; Tardugno, M.; Nebbioso, A.; Galmozzi, A.; Mitro, N.; De Fabiani, E.; Altucci, L.; Kazantsev, A. *J. Med. Chem.* **2009**, *52*, 5496.
(62) Azminah, A.; Erlina, L.; Radji, M.; Mun'im, A.; Syahdi, R. R.; Yanuar, A. *Comput. Biol. Chem.* **2019**, *83*, 107096.
(63) Manna, D.; Bhuyan, R.; Ghosh, R. *J. Mol. Model.* **2018**, *24*, 340.
(64) Schiedel, M.; Robaa, D.; Rumpf, T.; Sippl, W.; Jung, M. *Med. Res. Rev.* **2018**, *38*, 147.
(65) Peck, B.; Chen, C.-Y.; Ho, K.-K.; Di Fruscia, P.; Myatt, S. S.; Coombes, R. C.; Fuchter, M. J.; Hsiao, C.-D.; Lam, E. W. F. *Mol. Cancer Ther.* **2010**, *9*, 844.
(66) Promega, corporation. *SIRT-Glo™ Assay and Screening System. Technical Manual*; Promega Corporation: Madison, **2015**, 1–22.